© 2022 Journal of Pharmacy & Pharmacognosy Research, 10 (6), 1126-1138, 2022
ISSN 0719-4250
https://jppres.com

DOI: https://doi.org/10.56499/jppres22.1489_10.6.1126

*Original Article*

# Molecular simulation of compounds from *n*-hexane fraction of *Sonchus arvensis* L. leaves as SARS-CoV-2 antiviral through inhibitor activity targeting strategic viral protein

[Simulación molecular de compuestos de la fracción de n-hexano de las hojas de *Sonchus arvensis* L. como antivirales del SARS-CoV-2 a través de la actividad inhibidora dirigida a la proteína viral estratégica]

**Dwi Kusuma Wahyuni[1,2*], Sumrit Wacharasindhu[3], Wichanee Bankeeree[2], Hunsa Punnapayak[2], Hery Purnobasuki[1], Junairiah[1], Arif NM Ansori[4], Viol Dhea Kharisma[1,5], Arli Aditya Parikesit[6], Listyani Suhargo[1*], Sehanat Prasongsuk[1,2*]**

[1]Department of Biology, Faculty of Science and Technology, Universitas Airlangga Surabaya, East Java, 60115, Indonesia.
[2]Plant Biomass Utilization Research Unit, Department of Botany, Faculty of Science, Chulalongkorn University, Bangkok, 10330, Thailand.
[3]Department of Chemistry, Faculty of Science, Chulalongkorn University, Bangkok,10330, Thailand.
[4]Professor Nidom Foundation, Surabaya, East Java, 60115, Indonesia.
[5]Computational Virology Research Unit, Division of Molecular Biology and Genetics, Generasi Biologi Indonesia Foundation, Gresik, East Java, 61171, Indonesia.
[6]Department of Bioinformatics, School of Life Science, Indonesia International Institute for Life Sciences, Jakarta, 13210, Indonesia.
*E-mail: dwi-k-w@fst.unair.ac.id (DKW), listyani-s@fst.unair.ac.id (LS), sehanat.p@chula.ac.th (SP)

**Abstract**

*Context*: COVID-19 was caused by the spread and transmission of SARS-CoV-2 at the end of 2019 until now. The problem comes when antiviral drugs have not yet been found and patients infected with SARS-CoV-2 can trigger a cytokine storm condition due to the effects of viral replication. Indonesia has various kinds of medicinal plants, such as *Sonchus arvensis* L., which are used as medicinal plants.

*Aims*: To analyze the activity of the inhibitor as SARS-CoV-2 antiviral agents from *n*-hexane fractions of *S. arvensis* leaves.

*Methods*: The sample was collected from GC-MS analysis, PubChem, and Protein Databank database, then drug-likeness identification using Lipinski Rule of Five server and bioactive prediction of bioactive compounds as inhibitor activity was conducted by Molinspiration server. Furthermore, the docking simulation was performed using PyRx 0.9.9 software to determine the binding activity, molecular interaction by Discovery Studio software to identify position and interaction type, 3D molecular visualization by PyMol 2.5. software, and dynamic by CABS-flex 2.0 server to predict interaction stability.

*Results*: α-Amyrin and β-amyrin from *n*-hexane fractions of *S. arvensis* leaves had activity as SARS-CoV-2 inhibitors through interactions on helicase, RdRp, Mpro, and RBD-Spike, both compounds had more negative binding affinity than control drug and can produce stable chemical bond interactions in the ligand-protein complexes. However, the results were merely computational, so they must be validated through an *in vivo* and *in vitro* research approach.

*Conclusions*: *Sonchus arvensis* L. leaves were predicted to have SARS-CoV-2 antiviral through inhibitor activity by α-amyrin and β-amyrin.

*Keywords*: antiviral; bioinformatics; SARS-CoV-2; *Sonchus arvensis* L.

**Resumen**

*Contexto*: La propagación y la transmisión del SARS-CoV-2 han sido causadas por el COVID-19 desde finales de 2019 hasta ahora. El problema surge cuando aún no se han encontrado medicamentos antivirales y los pacientes infectados por el SARS-CoV-2 pueden desencadenar una condición de tormenta de citocinas debido a los efectos de la replicación viral. Indonesia tiene varios tipos de plantas medicinales, como *Sonchus arvensis* L., que se utilizan como plantas medicinales.

*Objetivos*: Analizar la actividad inhibidora de SARS-CoV-2 de fracciones de n-hexano de las hojas de *S. arvensis*.

*Métodos:* La muestra se recogió del análisis GC-MS, PubChem y la base de datos Protein Databank, luego se identificó la similitud de los fármacos utilizando el servidor Lipinski Rule of Five y se realizó la predicción de los compuestos bioactivos como actividad inhibidora mediante el servidor Molinspiration. Además, se realizó la simulación de acoplamiento mediante el software PyRx 0.9.9 para determinar la actividad de unión, la interacción molecular mediante el software Discovery Studio para identificar la posición y el tipo de interacción, la visualización molecular 3D mediante el software PyMol 2.5. y la dinámica mediante el servidor CABS-flex 2.0 para predecir la estabilidad de la interacción.

*Resultados*: La α-amirina y la β-amirina de las fracciones de n-hexano de las hojas de *S. arvensis* tuvieron actividad como inhibidores del SARS-CoV-2 a través de las interacciones en la helicasa, RdRp, Mpro y RBD-Spike, ambos compuestos tuvieron más afinidad de unión negativa que el fármaco de control y pueden producir interacciones de enlace químico estables en los complejos ligando-proteína. Sin embargo, los resultados fueron meramente computacionales, por lo que deben ser validados mediante un enfoque de investigación *in vivo* e *in vitro*.

*Conclusiones*: Se predijo que las hojas de *S. arvensis* tienen actividad antiviral contra el SARS-CoV-2 a través de la actividad inhibidora de la α-amirina y la β-amirina.

*Palabras Clave*: antiviral; bioinformática; SARS-CoV-2; *Sonchus arvensis* L.

ARTICLE INFO
Received: August 22, 2022.
Accepted: November 18, 2022.
Available Online: November 29, 2022.

AUTHOR INFO
ORCID: 0000-0002-1149-1103 (DKW)
0000-0002-1279-3904 (ANMA)
0000-0001-8716-3926 (AAP)
0000-0001-5617-1077 (SP)

## INTRODUCTION

SARS-CoV-2 is the main cause of the COVID-19 pandemic, which began at the end of 2019. This has caused several countries to go into lockdown to prevent the spread of the virus. The SARS-CoV-2 virus is transmitted through airborne particles, and each country's government requires everyone to wear a mask (Dhama et al., 2020). Since the end of 2019 until now, there has been no effective antiviral in treating SARS-CoV-2 infection in patients. Several control drugs, such as EIDD-2801 and PF-07321332, are used for the treatment of SARS-CoV-2, although they do not have definite scientific evidence. The drug EIDD-2801 or Molnupiravir is predicted to inhibit the replication process of SARS-CoV-2 during the budding phase, PF-07321332 or nirmatrelvir/ritonavir can interfere with the activity of viral protease enzymes (Ahmad et al., 2021; Singh et al., 2021). However, several studies revealed that the activity of EIDD-2801 and PF-07321332 decreased in efficacy due to several factors such as viral mutations that trigger unstrategic interaction positions and unstable bonds (Kabinger et al., 2021).

SARS-CoV-2 infection in humans can produce a cytokine storm condition due to the release of proinflammatory cytokines by immune cells, which can lead to death. Cells infected by SARS-CoV-2 consist of macrophages, epithelium, and dendrites (Murgolo et al., 2021). The virus infects cells by binding to the spike glycoprotein with the angiotensin-converting enzyme 2 (ACE-2) receptor (Bourgonje et al., 2020). Viruses have a specific enzyme called RNA-dependent RNA polymerase (RdRp), whose role is to trigger the catalysis of RNA replication reactions from the template. Other enzymes, such as helicase or NS13, also contribute to initiating the replication of viral genetic material (Maio et al., 2021). The polypeptides formed from protein synthesis will be cut by the Mpro enzyme into peptides to enter the assembly and budding stages of new viruses. SARS-CoV-2 antiviral drugs are designed to inhibit the activity of specific proteins that play a role in the viral replication process, such as glycoprotein, RdRp, Helicase, and Mpro (Shamsi et al., 2021).

In Indonesia, *Sonchus arvensis* L., a highly invasive species of the family *Asteraceae*, is used as a traditional medicinal plant for malaria treatment (Wahyuni et al., 2019; 2020a; 2021). This plant contains various active compounds, including flavonoids, saponins, and polyphenols (Delyan, 2016, Wahyuni et al., 2020b), which have been reported for moderate to high antioxidant (Khan, 2012), hepatoprotective (Hendriani et al., 2015), nephroprotective (Imelda et al., 2017), anti-inflammatory (Hendriani et al., 2015), and antibacterial activities (Rumondang et al., 2013). The aim of the present study was to analyze the inhibitory activity of SARS-CoV-2 antiviral agents from n-hexane fractions of *Sonchus arvensis* leaves.

## MATERIAL AND METHODS

### Plant material

*S. arvensis* was collected from Taman Husada Graha Famili (medicinal Plant Garden), Surabaya, Jawa Timur, Indonesia (7°18′12.2′′S 112°41′12.7′′7E). The plants were 2–3 months old (pre-generative stage). The leaves were green and apparently healthy, with no signs of destruction by insects or microbes. The plant material was confirmed as *S. arvensis* by the staff of the Purwodadi Botanical Garden (Pasuruan, East Java, Indonesia) operated by the Indonesian Institute of Sciences (Jakarta, Indonesia). A voucher specimen was deposited in the Plant Systematics Laboratory, Department of Biology, Faculty of Science and Technology, Universitas Airlangga, Surabaya City, East Java, Indonesia (No. SA.0110292021).

### Extraction

The leaves of S. *arvensis* were air-dried, ground into powder at room temperature, and macerated three times with *n*-hexane for 24 h each at room temperature. The liquid extract was filtered through Whatman no. 1 filter paper (pore diameter, 11 µm; Cytiva, Marlborough, MA, USA), then evaporated in a rotary evaporator at 60°C to acquire crude extracts, which were stored at 4°C for later use.

### Thin Layer Chromatography (TLC)

*n*-Hexane-extracted *S. arvensis* leaves (5 mg) were dissolved in *n*-hexane (100 µL), and 5 µL aliquots were spotted on a TLC plate (silica gel GF254; Sigma-Aldrich Corporation, St. Louis, MO, USA). Once dried, the TLC plate was developed with *n*-hexane and ethyl acetate (4:1), dried, sprayed with ρ-anisaldehyde sulfuric acid, and heated. Terpenoids on the TLC plate appeared as a purplish-blue node (Wahyuni et al., 2021).

### Purification and isolation

*n*-Hexane-extracted *S. arvensis* leaves were subjected to chromatography using a column (length, 80 cm length; cross-section, 2.5 cm) containing silica gel 60 (particle size, 0.063–0.200 mm; Merck KGaA, Darmstadt, Germany). The silica gel was weighed using a ratio of the adsorbent to extract of 80:10. A slurry of silica gel (80 g) was prepared with 100% *n*-hexane and

poured into the column. The crude extract (10 g) was dissolved in dichloromethane (10 mL) in a beaker and adsorbed in the silica gel (10 g). The mixture was stirred at room temperature until all the dichloromethane had evaporated and placed on top of a previously packed column. Initially, elution was conducted with 80% *n*-hexane and 20% ethyl acetate (Table 1). Fractions were collected in 10-mL Falcon™ bottles (Corning Inc., Corning, NY, USA) until the compounds were eluted entirely from the column. TLC fractions with the same Rf values were combined (Table 1).

**GC-MS analysis**

GC-MS analysis was used to determine the phytochemical profiles of *S. arvensis n*-hexane fractions 5–12 and 15–28. Each fraction (15 mL) was dissolved in chloroform (1 mL), then passed through a 45-µm filter. Triple quadrupole GC-MS/MS was performed with an Agilent 7890B GC system and Agilent 7633 ALS detector (Agilent Technologies, Inc., Santa Clara, CA, USA) with an Agilent J&W HP-5ms column (5% phenyl-methylpolysiloxane; inner diameter, 0.25 mm; length, 30 m; film thickness, 0.25 µm). The following settings were used for GC-MS analysis: flow rate of the mobile phase, 1 mL/min; average velocity, 36.445 cm/min; oven temperature, 40–320°C at 15°C/min and held for 3–20 min; post-run temperature, 320°C (2 mL/min) for 5 min; carrier gas, helium; flow rate of carrier gas, 29.75 mL/min; carrier flow rate, 1 mL/min (constant mode); sample volume, 10 µL; total running time, 24 min; injector temperature, 50°C; injection volume, 0.3 µL (fractions 15–28) or 1.8 µL (fractions, 5–12); split ratio, 20:1 (fractions 15–28) or 10:1 (fractions, 2–12); and inlet temperature, 280°C. The interface and mass spectra ion source was maintained at 320°C and 250°C, respectively. The mass spectra were collected at 70 eV with a mass scan range of 30–5550 amu, solvent delay of 3 min, and transfer line temperature of 320°C. The identification of compounds was based on comparing the mass spectra with those of the Standard Reference Database (National Institute of Standards and Technology/NIST version 02.L), Gaithersburg, MD, USA). The relative percentage of each component was calculated as the relative percentage of the total peak area of the chromatograph.

**Sample preparation of *in silico* anti-SARS-CoV-2 activity**

The GC-MS analysis of n-hexane fractions no. 15-28 of S. *arvensis* leave revealed α-amyrin (CID 73170), β-amyrin (CID 73145), betulin (CID 72326), lupeol (CID 259846), and taraxasterol (CID 441686). The COVID-19 drugs, EIDD-2801 or molnupiravir (CID 145996610 or Control 1) and PF-07321332 or paxlovid (CID 155903259 or Control 2), were as positive control. They were used as ligands in this study. The PubChem database (https://pubchem.ncbi.nlm.nih.gov/) was used to prepare samples of the selected chemical compounds in this study. The information obtained from this database consisted of ID, 3D structure, and canonical SMILES. The target proteins in this study consisted of helicase (PDB ID 6ZSL), RdRp (PDB ID 6M71), $M^{pro}$ (PDB ID), and RBD-spike (PDB ID 6LZG) in SARS-CoV-2, then the 3D structure of the protein was obtained from RCSB PDB (https://www.rcsb.org/), then sterilized native ligands and water through PyMol 2.5 version software with an academic license (Putra et al., 2020).

**Druglikeness identification**

Prediction of drug-like molecules of n-hexane fractions compounds of *S. arvensis* leaves was carried out according to Lipinski's Rule of Five (http://www.scfbio-iitd.res.in/software/drugdesign/lipinski.jsp). Prediction aimed to determine the ability of a chemical compound as a drug candidate by fulfilling parameters such as molecular weight, high lipophilicity (LogP), hydrogen donor bonds, acceptors, and molar refractivity. Natural drug-based candidates with drug-like molecule properties were predicted to show a high success rate in triggering target protein activity (Kharisma et al., 2022).

**Bioactivity prediction**

Prediction of inhibitory activity on the *n*-hexane fractions compounds of *S. arvensis* leaves was carried out via the Molinspiration v.2018.03 server (https://www.molinspiration.com/cgi-bin/properties). The prediction was made by referring to the bioactivity score, which is important in targeting drug binding, the bioactivity consisted of GPCR ligands, ion channel modulators, inhibitors, modulators, and nuclear receptors. Predictive scores with positive values indicated specific activities, such as inhibitors on query compounds (Shaheen et al., 2015).

**Molecular docking simulation**

This study used a molecular docking simulation method to determine the inhibitory ability of the ligand to the target protein (Prahasanti et al., 2021). The method used was a blind docking type. In this method, the functional side of the target protein was ignored, and only pays attention to the binding energy was formed because this method plays a role in screening ligand activity against the target protein

(Hassan et al., 2017; Kharisma et al., 2020). This study identified and predicted the mechanism of action of the *S. arvensis* compounds by binding to the inhibitory activity of the helicase protein, RdRp, Mpro, RBD-Spike in SARS-CoV-2. The docking simulation in this study was carried out using PyRx 0.9.9 version software with an academic license.

### Ligand-protein interaction and 3D visualization

The molecular complex resulting from the molecular docking simulation in this study was analyzed for the position and type of chemical bond interaction formed by the BIOVIA Discovery Studio 2017 version software. The software identified the types of weak bond interactions, such as hydrophobic, Van der Waals, hydrogen, electrostatic, and -alkyl, and displayed them in 2D (Ramos et al., 2022). The 3D structure of the molecular complex as the result of the molecular docking simulation in this study was displayed using PyMol 2.5 version software. The structure of the protein-ligand molecular complex consisted of cartoons, surfaces, and sticks and underwent a selection of staining.

### Molecular dynamic analysis

The stability of the binding interactions formed between ligands and specific domains in proteins was identified through molecular dynamics simulation with CABS-flex 2.0 version (http://biocomp.chem.uw.edu.pl/CABSflex2/index). The parameters used in this simulation consist of protein rigidity (1.0), protein restraints (ss2 3 3.8 8.0), global c-alpha restraints weight (1.0), global side-chain restraints weight (1.0), number of cycles (50), cycles between trajectory (50), temperature range (1.40), and RNG seed (227). The final result of the simulation is shown as a fluctuating graph, or root mean square fluctuation (RMSF), with a maximum distance of 1-3 Å (Wijaya et al., 2021).

### Data analysis

Data of this study were analyzed descriptively by comparing the result with the standard. The TLC data was analyzed by comparing the color of spot with standard (purple color: terpenoids) after sparyed by *ρ*-anisaldehyde sulfuric acid (Wahyuni et al., 2021). The spectra of GC-MS were verified by the data base spectra in the NIST version 02.L library. Furthermore, the *in silico* SARS-Cov-2 data was analyzed by software. The prediction of drug-like molecules was conducted with drugdesign software from scfbio (http://www.scfbio-iitd.res.in/software/drugdesign/lipinski.jsp). The PyRx 0.9.9 version software was used for molecular docking (Prahasanti et al., 2021). The BIOVIA Discovery Studio 2017 version software was used to analyze the position and type of chemical bond interaction (Kharisma et al., 2022). The CABS-flex 2.0 version (http://biocomp.chem.uw.edu.pl/CABSflex2/index) was performed using the molecular dynamic (Ramos et al., 2022).

## RESULTS

### Terpenoid screening of the *n*-hexane extract of *Sonchus arvensis* by TLC

The *n*-hexane extract of *S. arvensis* L. was analyzed by TLC using silica gel GF 254 as the stationary phase and *n*-hexane:ethyl acetate (4:1) as the mobile phase. There were two visible spots in daylight and under ultraviolet (UV) light at 254 nm (Rf value = 0.12 and 0.18). Under UV light at 366 nm, there were seven separate spots with Rf values of 0.14, 0.24, 0.29, 0.35, and 0.53. After staining with ρ-anisaldehyde sulfuric acid, three separate purple spots appeared, with Rf values of 0.31, 0.59, and 0.71 (Fig. 1).

### Isolation and purification

Sixty fractions were collected (Table 1). The TLC results of fractions 5–12 were notable and yellow crystals formed at the bottom of the falcon tubes of these samples. Further crystallization was induced using *n*-hexane at 4°C for 24 h. White crystals of the mother liquor had also formed at the bottom of the flasks. The light-yellow crystals were further purified by crystallization with *n*-hexane (white crystal, 198 mg). The yield of the final product was 1.98% (w/w).

Furthermore, the TLC results of fractions 15–28 were also significant. Brown crystals had formed at the bottom of the falcon tubes of these samples. Further crystallization was induced using n-hexane at 4°C for 24 h. Finally, 379 mg of white crystal was produced at a yield of 3.79%. The purity of each isolated compound was determined by TLC before spectral analysis.

### GC-MS analysis

GC-MS was used to determine the metabolite profile of two groups of *n*-hexane fractions of *S. arvensis* leaves: 5–12 and 15–28. Fractions 5–12 contained two compounds (stearyl palmitate and cetyl myristate) (Table 2, Fig. 2), while fractions 15–28 contained six (hexacosanol, β-amyrin, Lupeol, α-amyrin, betulin, and taraxasterol) (Table 3, Fig. 3). Octadecyl ester stearyl palmitate (fractions 5–12) and taraxasterol (fractions 15–28) were the major compounds among the eight detected.

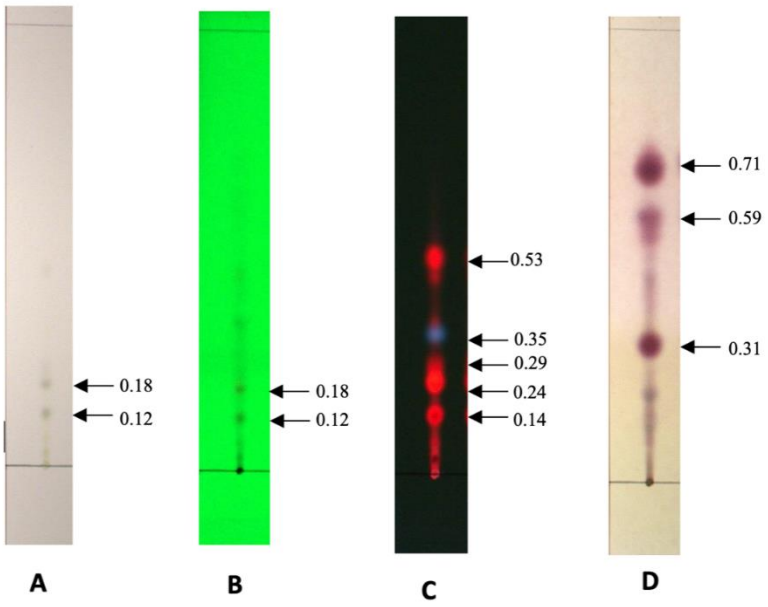


**Figure 1.** Chromatogram of *Sonchus arvensis* L. extract.

(A) Solvent only (*n*-hexane:ethyl acetate at 4:1 ). (B) UV light at 254 nm. (C) UV light at 366 nm. (D) Anisaldehyde sulfuric acid. The purple spot at 0.35 is a terpenoid.

**Table 1.** Column chromatographic separation of *Sonchus arvensis n*-hexane extract.

| Fractions | Solvent | Volume collected (mL) | Combined fractions | Rf values of major spots | Number of spots | TLC solvent (*n*-hexane:ethyl acetate) |
|---|---|---|---|---|---|---|
| 1–4 | *n*-Hexane | 40 | 1–4 | 0 | 0 | 4:1 |
| *5–12* | *n*-Hexane | 80 | *5–12* | 0.71 | 1 | 4:1 |
| 13–14 | *n*-Hexane | 20 | 13–14 | 0.71, 0.59, 0.31 | 3 | 4:1 |
| *15–28* | *n*-Hexane | 140 | *15–28* | 0.59, 0.31 | 2 | 4:1 |
| 29–35 | *n*-Hexane | 70 | 29–35 | 0.31, 0.24 | 2 | 4:1 |
| 36–60 | *n*-Hexane | 250 | 36–60 | 0.24, 1.8 | 1 | 4:1 |

Conditions for GC-MS are indicated in italics.

**Table 2.** Phytochemical components from GC-MS analysis of fractions 2-12 of *S. arvensis n*-hexane extract

| No | Compound | Retention Time (minutes) | Percentage of Area (%) | Bioactivity |
|---|---|---|---|---|
| 1 | Stearyl palmitate | 15.234 | 100 | Antimicrobial activities (Duke, 1992; Saito et al., 2006) |
| 2 | Cetyl myristate | 23.944 | 17 | Antimicrobial and antifeedant activities (Borg et al., 1987) |

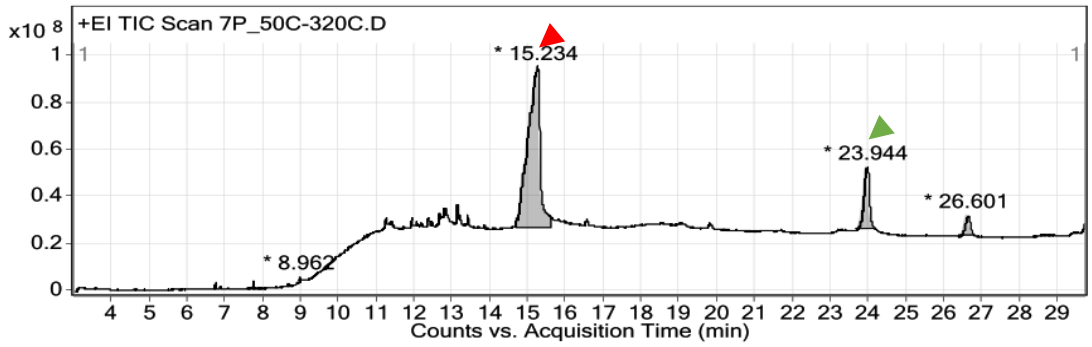


**Figure 2.** Representative chromatogram of fractions 5–12 of *Sonchus arvensis* L. *n*-hexane extract.
Red arrow, octadecyl ester hexadecanoic acid; green arrow, hexadecyl ester tetradecanoic acid.

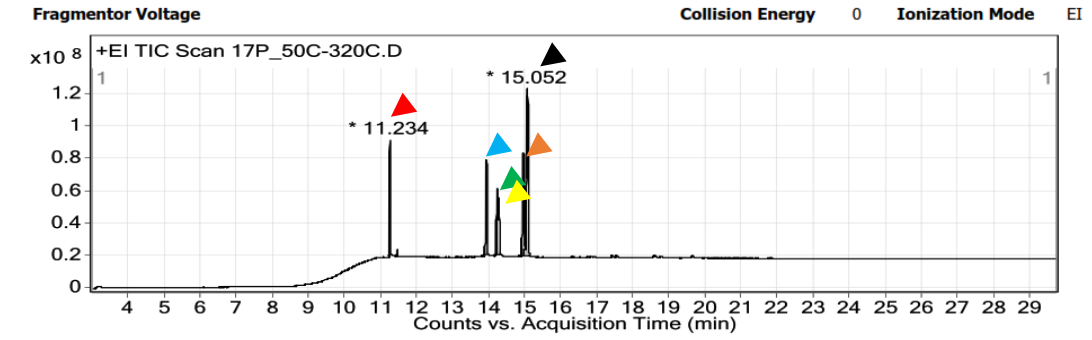


**Figure 3.** Representative chromatogram of fractions 15–28 of *Sonchus arvensis* L. *n*-hexane extract.
Red arrow, hexacosanol; blue arrow, β-amyrin; green arrow, lupeol; yellow arrow, α-amyrin; brown arrow, betulin; black arrow, taraxasterol.

**Table 3.** Phytochemical components from GC-MS analysis of fractions 15–28 of *S. arvensis n*-hexane extract.

| No | Compound | Retention time (minutes) | Percentage of area (%) | Bioactivities |
|---|---|---|---|---|
| 1 | Hexacosanol | 11.234 | 27.37 | Neurotrophic activities (Gade et al., 2017) |
| 2 | β-Amyrin | 13.911 | 43.41 | Antimicrobial (Ogwuche et al., 2014), antioxidant (Sunil et al., 2014) , and anti-inflamantory (Okoye et al., 2014) activities |
| 3 | Lupeol | 14.207 | 31.26 | Antimicrobial (Sunil et al., 2014), anti-inflammatory, and anti-arthritic (Okoye et al., 2014) activities |
| 4 | α-Amyrin | 14.255 | 25.91 | Antimicrobial activities (Biskup et al., 2019), stimulation of human keratinocytes (Niewolik et al., 2021) |
| 5 | Betulin | 14.965 | 59.51 | Anticancer activities (Tolstikov et al 2005) , drug delivery system (Tolstikov et al 2005), antiviral and antitumor agents (Sharma and Zafar, 2015) |
| 6 | Taraxasterol | 15.052 | 100 | Anticancer (Elnakady et al., 2017) and anti-edematous activities, lowers serum cholesterol levels (Widyananda et al., 2021) |

### *S. arvensis* compounds as drug-like molecule and inhibitor candidate

The five compounds were identified as drug-like by referring to the Lipinski Rule of Five parameters. Five compounds queried the leaf content of *S. arvensis* n-hexane fractions and acted as drug-like molecules or candidate drug molecules because they filled more than two of The Lipinski Rules of Five (Table 4). Five compounds containing *S. arvensis* leaves *n*-hexane fractions were categorized as drug-like molecules and probable to trigger specific activity when forming

complexes with target proteins. Prediction of inhibitor activity was carried out on five compounds of *n*-hexane fractions of *S. arvensis* leaves, which acted as drug-like molecules. The results showed that five compounds containing S. arvensis were probable inhibitors (Table 5).

**Revealing of *S. arvensis* compounds as an inhibitor**

The molecular docking simulation from PyRx 0.9.9 version software showed that the bioactive compounds from *n*-hexane fractions of S. *arvensis* leaves had the most negative binding affinity for each SARS-CoV-2 protein compared to drug control. The α-amyrin compound, when bound to the target protein helicase and RBD-spike, produced the lowest binding affinity, namely -9.8 kcal/mol and -8.3 kcal/mol, respectively. Then, the β-amyrin compound bound to RdRp and $M^{pro}$ produced the lowest binding affinity values, namely -9.0 kcal/mol and -8.3 kcal/mol, respectively (Table 6). The activity level of a candidate compound against the target protein was influenced by the binding affinity value formed on the molecular complex. The more negative meant the greater potential affected the target activity. The two compounds of *n*-hexane fractions of S. *arvensis* leave were predicted to affect the inhibitory response activity against the four target proteins because they have more negative binding affinity than other compounds and drug control. The two compounds could also act as dual inhibitors because each compound had the potential to inhibit each of two of the total four target proteins of SARS-CoV-2 (Table 6). The visualization of the docking simulation results was carried out in PyMol 2.5 version software with transparent surfaces, cartoon, and stick structures. Then the coloring selection was carried out based on the structure (Fig. 4).

The weak bond interactions formed in the docking complex consist of alkyl, hydrogen, hydrophobic, Van der Waals, and electrostatic interactions. The existence of weak binding interactions supported the existence of biological activity of proteins when there was ligand binding to specific domains. All bioactive compounds of *n*-hexane fractions of *S. arvensis* leaves bound to the target protein domain with weak binding interactions, consisting of alkyl, hydrogen, pi sigma, and Van der Waals (Table 7). These supported that each bioactive compound produced an inhibitory response to the target protein.

The stability of the binding to the molecular complex could be analyzed with molecular dynamic simulation by observing the fluctuating level based on the root mean square fluctuation (RMSF) value of each complex formed. The results showed that a stable complex was formed with the most negative lowest energy value having the highest RMSF value 4Å. The results of this study indicated that the RMSF of α-amyrin and β-amyrin at the pocket binding domain position of each target protein were stable and had a value of 4Å (Fig. 5).

**Table 4.** Druglikeness analysis of probability compounds from *n*-hexane fractions of *S. arvensis* leaves.

| Compound | MW (Dalton) | LOGP | HBD | HBA | MR | Probability |
|---|---|---|---|---|---|---|
| α-Amyrin | 426.000 | 8.024 | 1 | 1 | 130.649 | Drug-like molecule |
| β-Amyrin | 426.000 | 8.168 | 1 | 1 | 130.719 | Drug-like molecule |
| Lupeol | 426.000 | 8.025 | 1 | 1 | 130.670 | Drug-like molecule |
| Taraxasterol | 426.000 | 8.024 | 1 | 1 | 130.649 | Drug-like molecule |
| Betulin | 442.000 | 6.997 | 2 | 2 | 132.061 | Drug-like molecule |

**Table 5.** The prediction of inhibitor activity of *n*-hexane fractions of *S. arvensis* compounds.

| Compound | GPCR ligand | Inhibitors activity | | | Probabillity |
|---|---|---|---|---|---|
| | | Kinase | Protease | Enzyme | |
| α-Amyrin | 0.22 | 0.19 | -0.41 | 0.60 | Probable inhibitor |
| β-Amyrin | 0.22 | 0.11 | -0.31 | 0.56 | Probable inhibitor |
| Lupeol | 0.27 | 0.15 | -0.42 | 0.52 | Probable inhibitor |
| Taraxasterol | 0.17 | 0.08 | -0.23 | 0.50 | Probable inhibitor |
| Betulin | 0.21 | 0.09 | -0.41 | 0.51 | Probable inhibitor |

**Table 6.** Results of docking of *S. arvensis n*-hexane fraction compounds with SARS-CoV-2 protein.

| Target | Ligand | Grid positions (Å) | | Binding affinity (kcal/mol) |
|---|---|---|---|---|
| | | Center | Dimensions | |
| Helicase | α-Amyrin | X:-17,182 Y:30,909 Z:-74,684 | X:76,703 Y:96,531 Z:76,610 | -9.8 |
| | β-Amyrin | | | -9.4 |
| | Lupeol | | | -8.9 |
| | Taraxasterol | | | -9.3 |
| | Betulin | | | -8.8 |
| | EIDD-2801 (Control 1) | | | -6.8 |
| | PF-07321332 (Control 2) | | | -7.7 |
| RdRp | α-Amyrin | X:119,717 Y:123,605 Z:115,595 | X:79,274 Y:84,541 Z:95,129 | -8.6 |
| | β-Amyrin | | | -9.0 |
| | Lupeol | | | -7.9 |
| | Taraxasterol | | | -8.6 |
| | Betulin | | | -7.7 |
| | EIDD-2801 (Control 1) | | | -6.8 |
| | PF-07321332 (Control 2) | | | -7.0 |
| $M^{pro}$ | α-Amyrin | X:-26,256 Y:11,525 Z:58,967 | X:57,450 Y:69,117 Z:59,607 | -8.0 |
| | β-Amyrin | | | -8.3 |
| | Lupeol | | | -7.3 |
| | Taraxasterol | | | -8.0 |
| | Betulin | | | -7.3 |
| | EIDD-2801 (Control 1) | | | -6.7 |
| | PF-07321332 (Control 2) | | | -6.9 |
| RBD-Spike | α-Amyrin | X:212,130 Y:184,834 Z:203,765 | X:102,969 Y:99,563 Z:190,569 | -8.3 |
| | β-Amyrin | | | -8.2 |
| | Lupeol | | | -8.0 |
| | Taraxasterol | | | -8.1 |
| | Betulin | | | -7.0 |
| | EIDD-2801 (Control 1) | | | -6.2 |
| | PF-07321332 (Control 2) | | | -6.6 |

## DISCUSSION

Terpenoid screening of *n*-hexane extract revealed many spots. TLC is an established method for the separation of extracts of secondary metabolites of plant materials (Ali et al., 2017). The Rf value is an indicator of the diversity of terpenoid compounds separated from various extracts (Ahamed et al., 2017). Then GC-MS analysis showed several compounds that are known as bioactive compounds after comparing the spectra to the library. The fraction number 5-12 was identified as stearyl palmitate and cetyl myristate, which have antimicrobial activities (Aldakheel et al., 2020). Six compounds have existed in fraction number 15-28. Hexacosanol has a beneficial effect against detrusor overactivity in diabetic patients by ameliorating overexpression of muscarinic $M_2$ and $M_3$ receptor mRNAs (Borg et al., 1987), neurotrophic activity (Gade et al., 2017), and acetylcholinesterase inhibition activity in insects (Ogwuche et al., 2014). β-amyrin has antimicrobial (Sunil et al., 2014), antioxidant (Okoye et al., 2014), and anti-inflammatory activities. Lupeol has antimicrobial, anti-inflammatory, and anti-arthritic (Ekalu et al., 2019) activities. α-Amyrin has antimicrobial activities (Biskup et al., 2012) and stimulates human keratinocytes (So et al., 2018). Betulin has anticancer activities (Niewolik et al., 2021) and has been used as a drug delivery system (Tolstikov et al., 2005) and as antiviral and antitumor agent (Sharma et al., 2015). Taraxasterol has anticancer (Elnakady et al., 2017) and anti-

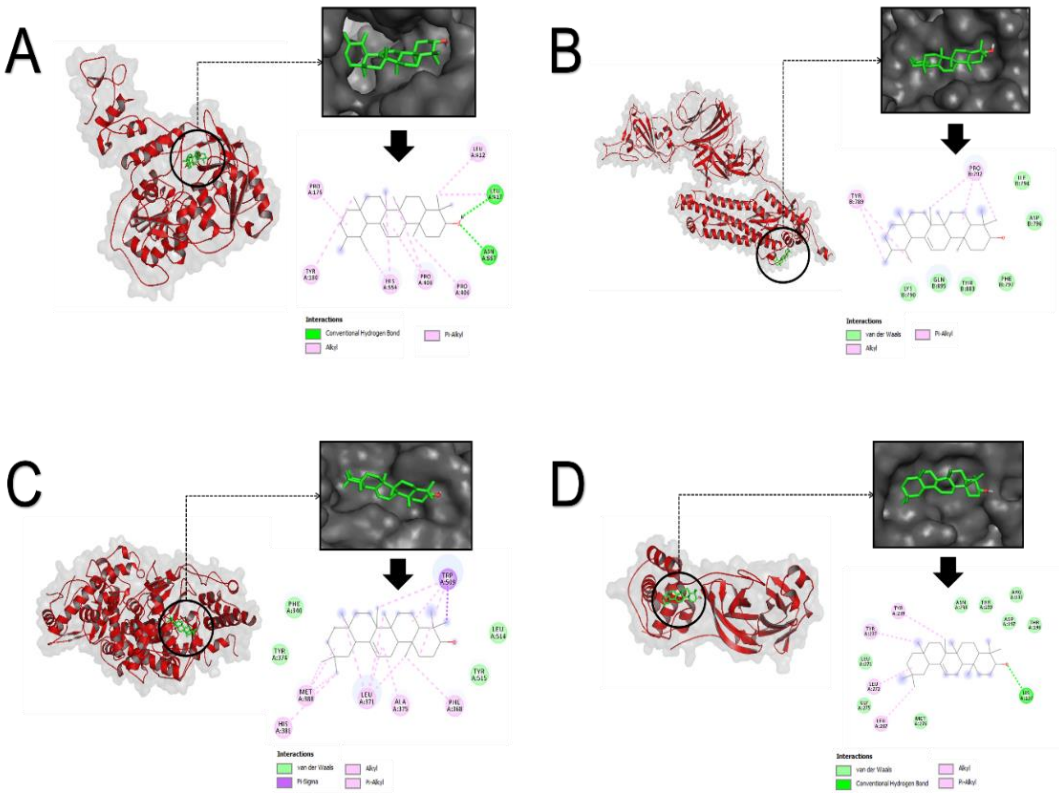


**Figure 4.** The 3D visualization of molecular docking results.
**(A)** α-Amyrin-Helicase; **(B)** α-Amyrin-Spike-RBD; **(C)** β-Amyrin-RdRp; and **(D)** β-Amyrin-M$^{pro}$.

**Table 7.** Results of docking of *S. arvensis n*-hexane fraction compounds with SARS-CoV-2 protein.

| Molecular complex | Molecular interaction |
|---|---|
| α-Amyrin_Helicase | Alkyl: Pro175, Tyr180, His554, Pro408, Pro406, Leu412<br>Hydrogen: Leu117, Asn557 |
| α-Amyrin_RBD-Spike | Alkyl: Tyr789, Pro792<br>Van der Waals: Ile794, Asp796, Lys790, Gln895, Thr883, Phe797 |
| β-Amyrin_RdRp | Alkyl: Met380, His381, Leu371, Ala375, His381<br>Pi Sigma: Trp509<br>Van der Waals: Phe340, Tyr374, Leu514, Tyr515 |
| β-Amyrin_M$^{pro}$ | Van der Waals: Leu271, Gly275, Met276, Asn238, Thr199, Asp197, Arg131, Thr198<br>Alkyl: Tyr239, Tyr237, Leu272, Leu287<br>Hydrogen: Lys137 |

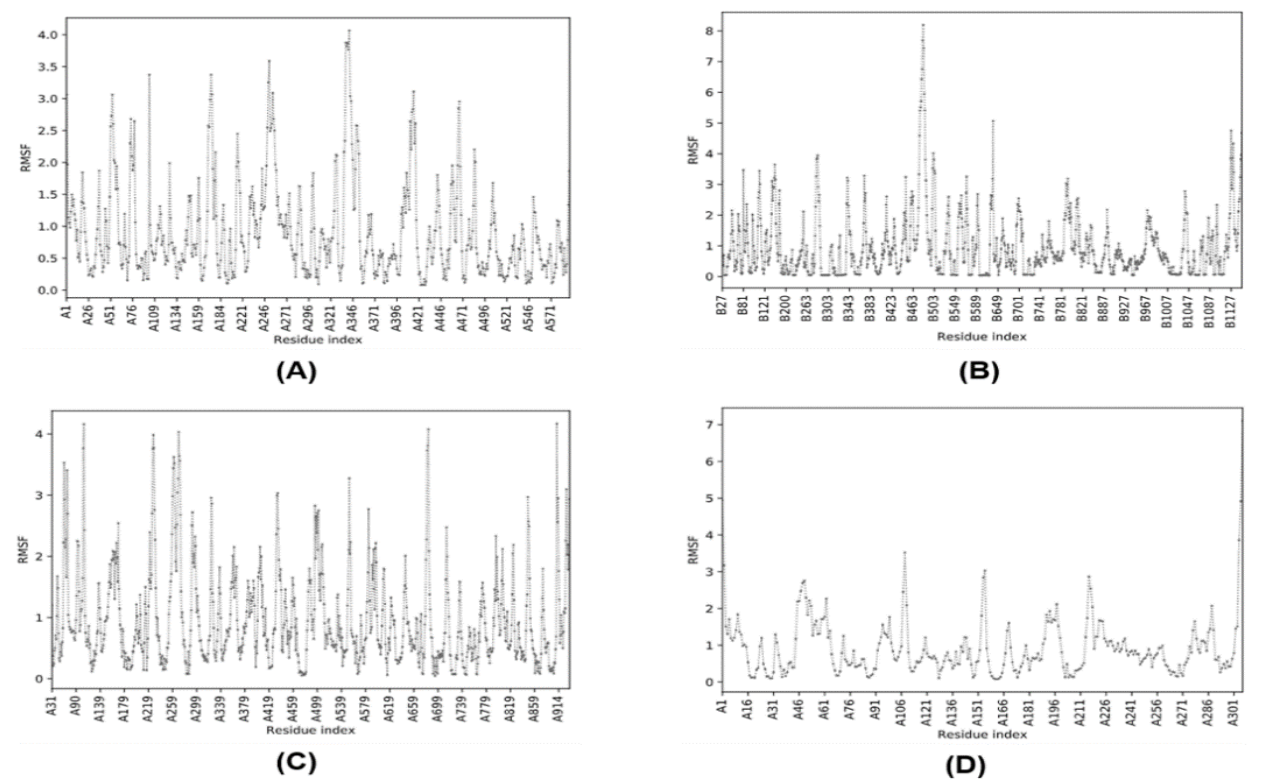


**Figure 5.** The root mean square fluctuation (RMSF) on protein-ligand complex.
**(A)** α-Amyrin-Helicase; **(B)** α-Amyrin-Spike-RBD; **(C)** β-Amyrin-RdRp; and **(D)** β-Amyrin-M$^{pro}$.

edematous activities and is reported to lower serum cholesterol levels (Widyananda et al., 2021).

A total of five compounds from fraction no 18-25 of the leaf of *S. arvensis n*-hexane extract acted as drug-like molecules and have probable inhibitor activity. Lipinski Rule of Five consists of molecular mass >500 Dalton, high lipophilicity <5, hydrogen bond donor <5, hydrogen bond acceptor <10. The Lipinski Rule of Five also plaid a role in predicting the ability of mobility to penetrate cell membranes and an early description of the effectiveness of the performance of query compounds (Benet et al., 2016; Ansori et al., 2021a). Prediction of inhibitor activity is obtained from the probability value of the query compound being an inhibitor when acting on the body of *Homo sapiens* (Ansori et al., 2021b). The types of inhibitor activity in this study were kinase, protease, and enzyme inhibitors. The positive prediction result of inhibitors for query compounds were shown by more positive probability values (Ansori et al., 2021c; Proboningrat et al., 2022).

This study uses docking to predict the mechanism of compounds from *S. arvensis* leaves when acting as SARS-CoV-2 antiviral. The blind docking method was used in this study to screen the activity of query compounds based on the level of binding affinity (Dibha et al., 2022). The activity of chemical compounds with inhibitory properties has a more negative binding affinity because it refers to Gibbs law, which shows the ability of ligand activity to trigger the target protein inhibition response (Du et al., 2016; Listiyani et al., 2022). The molecular docking results showed two compounds with the most potential as dual inhibitors, such as α-amyrin and β-amyrin. Furthermore, it has the ability to bind to the target with lower binding affinity. Moreover, the molecular complex could form weak bond interactions, which consist of hydrogen, hydrophobic, and π.

The docking results were then validated through molecular dynamic simulations, which aimed to determine the stability of the chemical bond interactions produced by the ligands in the target domain (Shivanika et al., 2022). Stability is indicated by the RMSF value, which refers to the fluctuating distance between the atoms making up the ligand and the amino acid residues of the protein domain where they interact with each other. The ideal RMSF value for the ligand-protein complex should be 1-3 Å to achieve stable bonding conditions (Wijaya et al., 2021). The molecular dynamic result showed α-amyrin and β-amyrin have RMSF value is >3 Å α-amyrin and β-amyrin from *n*-hexane fractions of *S. arvensis* leaves have activity as SARS-CoV-2 inhibitors through interactions on helicase, RdRp, M$^{pro}$, and RBD-Spike, both compounds have more negative binding affinity than control drug and can produce stable chemical bond

interactions in the ligand-protein complexes. However, the results are merely computational, so it must be validated through an *in vivo* and *in vitro* research approach.

## CONCLUSION

*Sonchus arvensis* L. leaves were predicted to have SARS-CoV-2 antiviral activity by α-amyrin and β-amyrin. Those two compounds strongly bound to helicase, RdRp, $M^{pro}$, and RBD-Spike, with a negative binding affinity more than the control drug and could produce stable chemical bond interactions in the ligand-protein complexes to trigger an inhibitory response. However, further studies or approaches are necessary to support the evidence-based results of this study.

## CONFLICT OF INTEREST

The authors declare no conflicts of interest.

## ACKNOWLEDGMENTS

This study was supported by Universitas Airlangga, Surabaya, Indonesia (Hibah COVID, Grant Number: 1056/UN3.15/PT/2021).

## REFERENCES

Ahamed T, Rahman SKM, Shohae AM (2017) Thin layer chromatographic profiling and phytochemical screening of six medicinal plants in Bangladesh. Int J Biosci 11(1): 131-140. https://doi.org/10.12692/ijb/11.1.131-140

Ahmad B, Batool M, Ain QU, Kim MS, Choi S (2021) Exploring the binding mechanism of PF-07321332 SARS-CoV-2 protease inhibitor through molecular dynamics and binding free energy simulations. Int J Mol Sci 22(17): 9124. https://doi.org/10.3390/ijms22179124

Aldakheel RK, Rehman S, Almessiere MA, Khan FA, Gondal MA, Mostafa A, Baykal A (2020) Bactericidal and *in vitro* cytotoxicity of *Moringa oleifera* seed extract and its elemental analysis using laser-induced breakdown spectroscopy. Pharmaceuticals 13(8): 193. https://doi.org/10.1101/2020.04.15.042663

Ali KS, Mohammed ASA, Munayem RT (2017) Phytochemical screening and thin layer chromatography of *Acacia etbaica* ssp. *uncinata* leaves. World J Pharm Res 6(12): 1278-1283. https://doi.org/10.20959/wjpr201712-9772

Ansori ANM, Fadholly A, Proboningrat A, Hayaza S, Susilo RJK, Naw SW, Posa GAV, Yusrizal YF, Sibero MT, Sucipto TH, Soegijanto S (2021a) *In vitro* antiviral activity of *Pinus merkusii* (Pinaceae) stem bark and cone against dengue virus type-2 (DENV-2). Res J Pharm Technol 14(7): 3705-3708. http://dx.doi.org/10.52711/0974-360X.2021.00641

Ansori ANM, Kharisma VD, Fadholly A, Tacharina MR, Antonius Y, Parikesit AA (2021b) Severe acute respiratory syndrome coronavirus-2 emergence and its treatment with alternative medicines: A review. Res J Pharm Technol 14(10): 5551-5557. https://doi.org/10.52711/0974-360X.2021.00967

Ansori ANM, Susilo RJK, Hayaza S (2021c) Biological activity investigation of phytocomponents in mangosteen (*Garcinia mangostana* L.): *in silico* study. Indian J Forensic Med Toxicol 15(1): 847-851. https://doi.org/10.37506/ijfmt.v15i1.13522

Benet LZ, Hosey CM, Ursu O, Oprea TI (2016) BDDCS, the rule of 5 and drugability. Adv Drug Deliv Rev 101:89-98. https://doi.org/10.1016/j.addr.2016.05.007

Biskup E, Golebiowski R, Stepnowski P, Lojkowska E (2012) Triterpenoid α-amyrin stimulates proliferation of human keratinocytes but does not protect them against UVB damage. Acta Biochim Pol 59(2): 255–260.

Borg J, Toazara J, Hietter H, Henry M, Schmitt G, Luu B (1987) Neurotrophic effect of naturally occurring long-chain fatty alcohols on cultured CNS. Neurons 213(2): 406-410. https://doi.org/10.1016/0014-5793(87)81531-4

Bourgonje AR, Abdulle AE, Timens W, Hillebrands JL, Navis GJ, Gordijn SJ, Bolling MC, Dijkstra G, Voors AA, Osterhaus AD, van der Voort PH, Mulder DJ, van Goor H (2020) Angiotensin-converting enzyme 2 (ACE2), SARS-CoV-2 and the pathophysiology of coronavirus disease 2019 (COVID-19). J Pathol 251(3): 228-248. https://doi.org/10.1002/path.5471

Delyan E (2016) Analysis of composition of volatile compounds of field sow thistle (*Sonchus arvensis* L.) leaves using the method of gas chromatography with mass-detection. J Pharm Innov 5: 118-121.

Dhama K, Khan S, Tiwari R, Sircar S, Bhat S, Malik YS, Singh KP, Chaicumpa W, Bonilla-Aldana DK, Rodriguez-Morales AJ (2020) Coronavirus disease 2019-COVID-19. Clin Microbiol Rev 33(4): e00028-20. https://doi.org/10.1128/CMR.00028-20

Dibha AF, Wahyuningsih S, Ansori ANM, Kharisma VD, Widyananda MH, Parikesit AA, Sibero MT, Probojati RT, Murtadlo AAA, Trinugroho JP, Sucipto TH, Turista DDR, Rosadi I, Ullah ME, Jakhmola V, Zainul R (2022) Utilization of secondary metabolites in algae *Kappaphycus alvarezii* as a breast cancer drug with a computational method. Pharmacog J 14(3): 536-543. https://doi.org/10.5530/pj.2022.14.68

Du X, Li Y, Xia YL, Ai SM, Liang J, Sang P, Ji XL, Liu SQ (2016). Insights into protein-ligand interactions: mechanisms, models, and methods. Int J Mol Sci 17(2): 144. https://doi.org/10.3390/ijms17020144

Duke JA (1992) Handbook of phytochemical constituents of GRAS herbs and other economic plants, CRC Press, Boca Raton, FL, USA.

Ekalu A, Ayo RGO, Habila JD, Hamisu (2019) Bioactivities of phaeophytin a, α-amyrin, and lupeol from *Brachystelma togoense* Schltr. J Turk Chem Soc 6(3): 411-418. https://doi.org/10.18596/jotcsa.571770

Elnakady YA, Rushdi AI, Franke R, Abutaha N, Ebaid H, Baabbad M, Omar MOM, Al Ghamdi AA (2017) Characteristics, chemical compositions and biological activities of propolis from Al-Bahah, Saudi Arabia. Sci Rep 7: 41453. https://doi.org/10.1038/srep41453

Gade S, Rajamanikyam M, Vadlapudi V, Nukala MK, Aluvala R, Giddigari C, Karanam NJ, Barua NC, Pandey R, Upadhayayula VSV, Srpadi P, Amanchy R, Upadhyayula SM (2017) Acetylcholinesterase inhibitory activity of stigmasterol & hexacosanol is responsible for larvicidal and repellent properties of *Chromolaena odorata*. Biochim Biophys Acta 1861(3): 541-550. https://doi.org/10.1016/j.bbagen.2016.11.044

Hassan NM, Alhossary AA, Mu Y, Kwoh CK (2017) Protein-ligand blind docking using QuickVina-W with inter-process spatio-temporal integration. Scie Rep 7(1): 15451. https://doi.org/10.1038/s41598-017-15571-7

Hendriani R, Sukandar EY, Anggadiredja K. Sukrasno (2015) *In vitro* evaluation of xanthine oxidase inhibitory activity of selected medicinal plants. Int J Pharm Clin 8: 235-238.

Imelda I, Azaria C, Lucretia T (2017) Protective effect of ethanol extract tempuyung leaf (*Sonchus arvensis* L.) against gentamicin induced renal injury viewed from blood ureum

level. Med Health 1: 575-82. https://doi.org/10.28932/jmh.v1i6.555

Kabinger F, Stiller C, Schmitzová J, Dienemann C, Kokic G, Hillen HS, Höbartner C, Cramer P (2021) Mechanism of molnupiravir-induced SARS-CoV-2 mutagenesis. Nat Struct Mol Biol 28(9): 740-746. https://doi.org/10.1038/s41594-021-00651-0

Khan RA (2012) Evaluation of flavonoids and diverse antioxidant activities of *Sonchus arvensis*. Chem Cent J 6(1): 126. https://doi.org/10.1186/1752-153X-6-126

Kharisma VD, Agatha A, Ansori ANM, Widyananda MH, Rizky WC, Dings TGA, Derkho M, Lykasova I, Antonius Y, Rosadi I, Zainul R (2022) Herbal combination from *Moringa oleifera* Lam. and *Curcuma longa* L. as SARS-CoV-2 antiviral via dual inhibitor pathway: A viroinformatics approach. J Pharm Pharmacogn Res 10(1): 138–146. https://doi.org/10.56499/jppres21.1174_10.1.138

Kharisma VD, Ansori ANM, Nugraha AP (2020) Computational study of ginger (*Zingiber officinale*) as E6 inhibitor in human papillomavirus type 16 (HPV-16) infection. Biochem Cell Arch 20 (Suppl 1): 3155-3159. https://doi.org/10.35124/bca.2020.20.S1.3155

Listiyani P, Kharisma VD, Ansori AN, Widyananda MH, Probojati RT, Murtadlo AA (2022) *In silico* phytochemical compounds screening of *Allium sativum* targeting the Mpro of SARS-CoV-2. Pharmacog J 14(3): 604-609. https://10.5530/pj.2022.14.78

Maio N, Lafont BAP, Sil D, Li Y, Bollinger JM Jr, Krebs C, Pierson TC, Linehan WM, Rouault TA (2021) Fe-S cofactors in the SARS-CoV-2 RNA-dependent RNA polymerase are potential antiviral targets. Science 373(6551): 236-241. https://doi.org/10.1126/science.abi5224

Murgolo N, Therien AG, Howell B, Klein D, Koeplinger K, Lieberman LA, Adam GC, Flynn J, McKenna P, Swaminathan G, Hazuda DJ, Olsen DB (2021) SARS-CoV-2 tropism, entry, replication, and propagation: considerations for drug discovery and development. PLoS Pathog 17(2): e1009225. https://doi.org/10.1371/journal.ppat.1009225

Niewolik D, Bednarczyk-Cwynar B, Ruszkowsk P, Sosnowski TR, Jaszcz K (2021) Bioactive betulin and PEG based polyanhydrides for use in drug delivery systems. Int J Mol Sci 22(3): 1090. https://doi.org/10.3390/ijms22031090

Ogwuche CE, Amupitan JO, Ayo RG (2014) Isolation and biological activity of the triterpene ß-amyrin from the aerial plant parts of *Maesobotrya barteri* (Baill). Med Chem 4: 729–733. https://doi.org/10.4172/2161-0444.1000221

Okoye NN, Ajaghaku DL, Okeke HN, Ilodigwe EE, Nworu CS, Okoye FBC (2014) Beta-amyrin and alpha-amyrin acetate isolated from the stem bark of *Alstonia boonei* display profound anti-inflammatory activity. Pharm Biol 52: 1478–1486. https://doi.org/10.3109/13880209.2014.898078

Prahasanti C, Nugraha AP, Kharisma VD, Ansori ANM, Devijanti R, Ridwan TPSP, Ramadhani NF, Narmada IB, Ardani IGAW, Noor TNEBA (2021) A bioinformatic approach of hydroxyapatite and polymethylmethacrylate composite exploration as dental implant biomaterial. J Pharm Pharmacog Res 9(5): 746-754. https://doi.org/10.56499/jppres21.1078_9.5.746

Proboningrat A, Kharisma VD, Ansori ANM, Rahmawati R, Fadholly A, Posa GAV, Sudjarwo SA, Rantam FA, Achmad AB (2022) *In silico* study of natural inhibitors for human papillomavirus-18 E6 protein. Res J Pharm Technol 15(3): 1251-1256. https://doi.org/10.52711/0974-360X.2022.00209

Putra WE, Kharisma VD, Susanto H (2020) Potential of *Zingiber officinale* bioactive compounds as inhibitory agent against the IKK-B. AIP Conf Proc 2231(1): 040048. https://doi.org/10.1063/5.0002478

Ramos RS, Borges RS, de Souza JSN, Araujo IF, Chaves MH, Santos CBR (2022) Identification of potential antiviral inhibitors from hydroxychloroquine and 1,2,4,5-tetraoxanes analogues and investigation of the mechanism of action in SARS-CoV-2. Int J Mol Sci 23(3): 1781. https://doi.org/10.3390/ijms23031781

Rumondang M, Kusrini D, Fachriyah E (2013) Isolation, identification and antibacterial test of triterpenoid compounds from *n*-hexane extract of tempuyung leaves (*Sonchus arvensis* L.). Pharm Sci 05: 506-507.

Saito M, Kinoshita Y, Satoh I, Bex A, Bertaccini A (2006) Ability of cyclohexenonic long-chain fatty alcohol to reverse diabetes-induced cystopathy in the rat. Eur Urol 51(2): 479-488. https://doi.org/10.1016/j.eururo.2006.06.024

Shaheen U, Akka J, Hinore JS, Girdhar A, Bandaru S, Sumithnath TG, Nayarisseri A, Munshi A (2015) Computer aided identification of sodium channel blockers in the clinical treatment of epilepsy using molecular docking tools. Bioinformation 11(3): 131-137. https://doi.org/10.6026/97320630011131

Shamsi A, Mohammad T, Anwar S, Amani S, Khan MS, Husain FM, Rehman MT, Islam A, Hassan MI (2021) Potential drug targets of SARS-CoV-2: From genomics to therapeutics. Int J Biol Macromol 177: 1-9. https://doi.org/10.1016/j.ijbiomac.2021.02.071

Sharma K, Zafar R (2015) Occurrence of taraxerol and taraxasterol in medicinal plants. Pharmacog Rev 9(17): 19-23. https://doi.org/10.4103/0973-7847.156317

Shivanika C, Deepak KS, Venkataraghavan R, Pawan T, Sumitha A, Brindha DP (2022) Molecular docking, validation, dynamics simulations, and pharmacokinetic prediction of natural compounds against the SARS-CoV-2 main-protease. J Biomol Struct Dyn 40(2): 585-611. https://doi.org/10.1080/07391102.2020.1815584

Singh AK, Singh A, Singh R, Misra A (2021) Molnupiravir in COVID-19: A systematic review of literature. Diabetes Metab Syndr 15(6): 102329. https://doi.org/10.1016/j.dsx.2021.102329

Sunil C, Irudayaraj SS, Duraipandiyan V, AlDhabi NA, Agastian P, Ignacimuthu S (2014) Antioxidant and free radical scavenging effects of ß-amyrin isolated from *S. cochinchinensis* Moore. leaves. Ind Crops Prod 61: 510–516. https://doi.org/10.1016/j.indcrop.2014.07.005

Tolstikov GA, Flekhter OB, Shultz EE, Baltina LA, Tolstikov AG (2005) Betulin and its derivatives. Chemistry and biological activity. Chem Sustainable Dev 13: 1-29.

Wahyuni DK, Lestari S, Kuncoro EP, Purnobasuki H (2020b) Callus induction and its metabolite profiles of *Sonchus arvensis* L. under temperature treatment. Ann Biol 36(2): 299–303.

Wahyuni DK, Purnobasuki H, Kuncoro EP, Ekasari W (2020a) Callus induction of *Sonchus arvensis* L. and its antiplasmodial activity. Afr J Infect 14: 1-7. https://doi.org/10.21010/ajid.v14i1.1

Wahyuni DK, Rahayu S, Purnama PR, Saputro TB, Suharyanto, Wijayanti N (2019) Morpho-anatomical structure and DNA barcode of *Sonchus arvensis* L. Biodiversitas 20(24): 17-26. https://doi.org/10.13057/biodiv/d200841

Wahyuni DK, Rahayu S, Zaidan AH, Ekasari W, Prasongsuk S, Purnobasuki H (2021) Growth, secondary metabolite production, and *in vitro* antiplasmodial activity of *Sonchus arvensis* L. callus under dolomite [CaMg(CO3)2] treatment. PLoS One 16: e0254804. https://doi.org/10.1371/journal.pone.0254804

Widyananda MH, Pratama SK, Samoedra RS, Sari FN, Kharisma VD, Ansori ANM, Antonius Y (2021) Molecular docking study of sea urchin (*Arbacia lixula*) peptides as multi-target inhibitor for non-small cell lung cancer (NSCLC) associated proteins. J

Pharm Pharmacog Res 9(4): 484-496. https://doi.org/10.56499/jppres21.1047_9.4.484

Wijaya RM, Hafidzhah MA, Kharisma VD, Ansori ANM, Parikesit AA (2021) COVID-19 *in silico* drug with *Zingiber officinale* natural product compound library targeting the Mpro protein. Makara J Sci 25(3): 162-171. https://doi.org/10.7454/mss.v25i3.1244

**AUTHOR CONTRIBUTION:**

| Contribution | Wahyuni DK | Wacharasindhu S | Bankeeree W | Punnapayak H | Parikesit AA | Kharisma VD | Ansori ANM | Suhargo L | Prasongsuk S |
|---|---|---|---|---|---|---|---|---|---|
| Concepts or ideas | x | | | x | x | | | x | x |
| Design | x | | | | | | | x | x |
| Definition of intellectual content | x | x | x | x | x | | | x | x |
| Literature search | x | x | | | | | x | x | x |
| Experimental studies | x | | | | | | x | x | x |
| Data acquisition | x | x | x | x | x | x | x | x | x |
| Data analysis | x | | | x | x | x | x | x | x |
| Statistical analysis | x | | | | | | x | x | x |
| Manuscript preparation | x | | | | | | x | x | x |
| Manuscript editing | x | x | x | x | | | x | x | x |
| Manuscript review | x | x | x | x | x | x | x | x | x |

**Citation Format:** Wahyuni DK, Wacharasindhu S, Bankeeree W, Punnapayak H, Parikesit AA, Kharisma VD, Ansori ANM, Suhargo L, Prasongsuk S (2022) Molecular simulation of compounds from *n*-hexane fraction of *Sonchus arvensis* L. leaves as SARS-CoV-2 antiviral through inhibitor activity targeting strategic viral protein. J Pharm Pharmacogn Res 10(6): 1126–1138. https://doi.org/10.56499/jppres22.1489_10.6.1126